Engineering Notes

ENGINEERING NOTES are short manuscripts describing new developments or important results of a preliminary nature. These Notes cannot exceed 6 manuscript pages and 3 figures; a page of text may be substituted for a figure and vice versa. After informal review by the editors, they may be published within a few months of the date of receipt. Style requirements are the same as for regular contributions (see inside back cover).

Quantum Statistical Analysis of Surface Sputtering

H. E. Wilhelm*
Colorado State University, Fort Collins, Colo.

Introduction

AT sufficiently low energies of the incident ions, exclusively surface atoms of the solid are sputtered. The experimental data on sputtering of metal surfaces indicate that the average number $S(E)$ of atoms sputtered per incident ion of energy E lies in the interval[1]

$$O \leq S(E) < 1, \quad E_0 \leq E < 10^2 eV \tag{1}$$

where E_0 is the threshold energy for sputtering of surface atoms. The measured $S(E)$-curves can be fitted by analytical expressions of the form[2]

$$S(E) = a(E - E_0)^n, \quad a = \text{const}, \; n = 2 \tag{2}$$

at low energies, $E_0 \leq E < 10^2 ev$. It is shown that this sputtering formula can be explained theoretically by means of a 3-body sputtering mechanism involving the ion and two surface atoms of the solid. By means of a quantum-statistical analysis, one finds independently that $n = 2$ and that "a" is a weak function of energy E which can be taken to be a constant for $E \gtrsim E_0$, i.e., $a(E) \cong a(E_0)$.

The theory to be presented is of interest for the evaluation of the surface sputtering observed at the cathodes of thruster and neutralizer discharges and on the accelerating grid of ion propulsion systems.[3,4]

Theory and Application

An ordinary binary collision between a surface atom of the solid and an ion incident normal to the surface can evidently not lead to sputtering since the atom does not acquire a momentum component in the direction of the external normal of the surface. Similarly, sputtering is not likely to occur for smaller angles of ion incidence if its energy is not large compared to the threshold energy for sputtering. It is evident that sputtering, at ion energies of the order of the threshold energy, is a 3-body process involving one ion and two surface atoms of the solid. At higher ion energies, however, sputtering will result mainly from higher order many-body interactions.

By restricting the theoretical considerations to ion energies E of the order of the threshold energy E_0, $E_0 \leq E < 10^2 eV$, sputtering is regarded as the result of an ion-atom-atom-interaction. Furthermore, it is assumed that the solid is polycrystalline and has a sublimination energy $E_s = \langle E_s(ijk) \rangle$ where the average is taken over the randomly distributed surfaces (ijk) of the crystallites. In this case, the sublimation energy E_s represents the average binding energy of a surface atom. In the 3-body sputtering process, the incident ion transfers, on the average, the energy E_s(as well as kinetic energy) to the atom which is expelled and the energy α) $2E_s$ or β) $4E_s$ to the other atom depending on whether the latter is pushed to an α) unstable or β) stable interstitial lattice position. Accordingly, the threshold energies for the 3-body interactions α) and β) are

$$E_0 = E_\alpha \equiv E_s + 2E_s = 3E_s \tag{3}$$

$$E_0 = E_\beta \equiv E_s + 4E_s = 5E_s \tag{4}$$

Depending on whether the process α) or β) occurs with dominant probability, the apparent threshold (obtained by extrapolation of the experimental $S(E)$-curve, $E \to E_0$) will be α) $E_0 \simeq E_\alpha$ or β) $E_0 \simeq E_\beta$. In the intermediate case γ), the threshold appears to be given by the dislocation energy[1] E_γ

$$E_0 = E_\gamma \equiv 4E_s \tag{5}$$

For example, the experimental thresholds[2] of Pt, Ta, Zr correspond to $E_0 = 3E_s$, those of Co, Cu, Ti correspond to $E_0 = 5E_s$, and those of Mo, Nb, W correspond to $E_0 = 4E_s$. In Table 1, the experimentally observed threshold energies E_0 of Mo and W are compared with the theoretical values of E_0 which lie well within the experimental uncertainties. In accord with the theoretical conceptions, the experimental results indicate that the true sputtering threshold E_0 is a material constant which is independent of the mass ratio of the atom and ion.[2]

When an ion of low energy as defined above hits the surface of a solid, the most likely interactions to occur are: 1) the ion is scattered without energy loss by the surface atom it encounters; 2) the ion collides with a surface atom and quasi-simultaneously with a second atom so that 3-body sputtering results. (More precisely, the designation "atom" should be used for the incident "ion" since the latter recombines with an electron as it approaches the surface of the solid.) The total probability for the ion to interact in either of the two ways with the solid is

$$P_N = N^{2/3} \sigma(E) \tag{6}$$

where N is the number density of atoms in the solid and $\sigma(E)$ is the total (energy dependent) cross section for ion-atom scattering. Let $W_1(E)$ and $W_2(E)$ be the probabilities for the processes 1) and 2), respectively. The relative probability with which sputtering occurs is then

$$W_s(E) = \frac{W_2(E)}{W_1(E) + W_2(E)} \cong \frac{W_2(E)}{W_1(E)}, \quad W_2(E) \ll W_1(E) \tag{7}$$

Combining of Eqs. (6) and (7) yields for the sputtering rate, i.e., the number of atoms expelled on the average by one ion

Table 1 Experimental and theoretical threshold energies

Metal	E_0(exper) *ev*	E_s *ev*	$E_0 = 4E_s$ *ev*
Mo	24	6.2	24.8
W	35	8.8	35.2

Received March 7, 1975. Presented as Paper 75-401 at the AIAA 11th Electrical Propulsion Conference, New Orleans, La., March 19-20, 1975; revision received November 14, 1975. This work was supported by NASA.

Index categories: Electric and Advanced Space Propulsion; Material Ablation.

*Professor of Electrical Engineering, Department of Electrical Engineering.

of energy E from the solid

$$S(E) = \sigma(E) N^{2/3} W_s(E) \tag{8}$$

In the processes 1) or 2), the ion interacts with the surface of the solid within an area of the extension of the de Broglie wavelength, $\lambda = \hbar (2mE)^{-1/2}$. For this reason, the spatial part of the phase space is taken to be

$$V = \frac{4\pi}{3} R^3, \quad R \cong \hbar / (2mE)^{1/2} \tag{9}$$

The probability for transition into a final state is proportional to i) the probability w that the interacting particles are simultaneously within V and ii) the density of final states $d\rho/dE$ per unit energy. For a state containing n independent particles with momenta $p_1, p_2, \ldots, p_n$, w and $d\rho/dE$ are given by

$$w = \left(\frac{V}{\Omega} \right)^n, \quad \frac{d\rho}{dE} = \left[\frac{\Omega}{(2\pi\hbar)^3} \right]^n \frac{d\Phi(E)}{dE} \tag{10}$$

Ω designates the normalization volume, $\Omega > V$, and $\Phi(E)$ is the volume of momentum space corresponding to the total energy E. Accordingly, the probability for transition into the final state n under consideration is

$$W(E) \propto [V/(2\pi\hbar)^3]^n \frac{d\Phi(E)}{dE} \tag{11}$$

$W_1(E)$ is defined as the probability for the ion to be scattered at the surface of the solid without energy loss. In the center of mass system, the ion momentum is $p = (2mE)^{1/2}$ in the final state and the momentum space volume is $\Phi(E) = 4\pi p^3/3$. According to Eq. 11, the probability for elastic scattering is $(n = 1)$

$$W_1(E) \propto [V/(2\pi\hbar)^3]^1 4\pi\sqrt{2} m^{3/2} E^{1/2} \tag{12}$$

$W_2(E)$ is defined as the probability for the 3-body sputtering state. In the center of mass system, the momenta of the ion i, the sputtered atom s, and the second atom a can be chosen as

$$p_i = p, \; p_s = -\tfrac{1}{2} p - q, \quad p_a = -\tfrac{1}{2} p + q \tag{13}$$

so that momentum is conserved, $\Sigma_j p_j = 0$. Since the threshold energy E_0 is expended in the sputtering interaction, the total kinetic energy of the three particles is

$$E^* = E - E_0 = \left(\frac{1}{2m} + \frac{1}{4M} \right) p^2 + \frac{1}{M} q^2 \tag{14}$$

Hence the volume of the momentum space is

$$\Phi(E) = \frac{\pi^3}{6} \left(\frac{4mM^2}{m+2M} \right)^{3/2} E^{*3} \tag{15}$$

Owing to conservation of momentum, only two of the particle momenta are independent, i.e., $n = 2$. Substitution of Eq. (15) into Eq. (11) gives for the probability of the sputtering state

$$W_2(E) \propto [V/(2\pi\hbar)^3]^2 \, 4\pi^3 \left(\frac{mM^2}{m+2M} \right)^{3/2} E^{*2} \tag{16}$$

With the assumption $W_1(E) \gg W_2(E)$, one obtains from Eqs. (9), (12), and (16) for the relative sputtering probability (if the anisotropy coefficients in W_1 and W_2 are about equal)

$$W_s(E) \cong \frac{1}{24} \left[\frac{(M/m)^2}{1+2(M/m)} \right]^{3/2} \frac{(E-E_0)^2}{E^2} \tag{17}$$

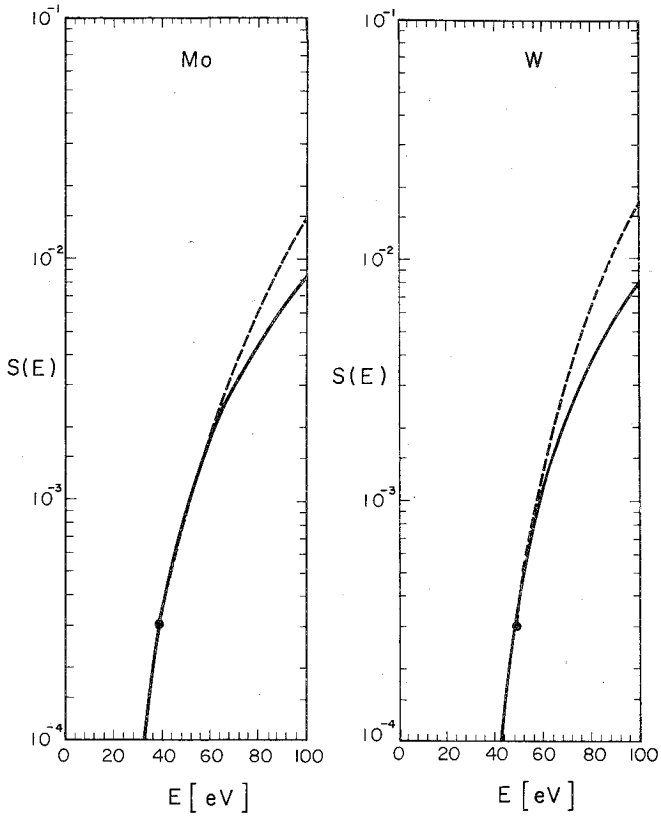

Fig. 1 Theoretical (——) and experimental (– – –) sputtering ratios $S(E)$ for Mo and W.

This result may be further simplified for ion energies close to the threshold, $E \gtrsim E_0$

$$W_s(E) \cong \frac{1}{24} \left[\frac{(M/m)^2}{1+2(M/m)} \right]^{3/2} \frac{(E-E_0)^2}{E_0^2} \tag{18}$$

Combining of Eqs. (8) and (17) yields for number $S(E)$ of atoms M squttered on the average by an ion m of energy $E \gtrsim E_0$ the expression $[\sigma(E)/E^2 \cong \sigma(E_0)/E_0^2]$

$$S(E) \cong \frac{1}{24} \sigma(E_0) N^{2/3} \left[\frac{(M/m)^2}{1+2(M/m)} \right]^{3/2} \frac{(E-E_0)^2}{E_0^2}$$

$$E \gtrsim E_0 \tag{19}$$

In the following, Eq. (19) is used to predict the sputtering ratios $S(E)$ for mercury ions (Hg) and molybdenum and wolfram targets. The sputtering rates for the latter cases are of direct interest for the evaluation of sputtering damage on accelerating grids[3] and the deposition of sputtering products on system components.[4] The theoretical threshold energies $E_0 = 4E_s$ for the metals Mo and W are given in Table 1. The remaining particle constants in Eq. (19), the masses M, the atom densities N, and the cross sections $\sigma(E_0)$ for Mo and W are given in Table 2[5] ($m \equiv m_{Hg} = 3.329 \times 10^{-22}$gr). The cross sections $\sigma(E_0)$ are estimates obtained from cross section data of atoms with similar atomic structure, since cross section values for Hg—Mo, Hg—W scattering at low energy are not available.[6]

Table 2 Constants for polycrystalline Mo and W ($m \equiv m_{Hg}$)

	M[gr]	M/m	N[cm^{-3}]	$\sigma(E_0)$ [cm^2]
Mo	1.592×10^{-22}	4.783×10^{-1}	6.418×10^{22}	3.4×10^{-16}
W	3.052×10^{-22}	9.655×10^{-1}	6.325×10^{22}	2.2×10^{-16}

In Fig. 1, the theoretical (——)sputtering rates $S(E)$ are plotted in dependence of energy $E_0 < E \leq 100$ eV for Hg ions, and W and Mo targets. For comparison, the corresponding experimental (– – –) sputtering ratios $S(E)$ as measured by Askerov and Sena[7] are shown, which represent the most reliable sputtering data presently available. It is seen that the agreement between theory and experiment is very satisfactory for energies E close to the threshold E_0. In view of the approximations made, it is clear that the theoretical and experimental $S(E)$ values must deviate more and more for increasing E. A better agreement between theory and experiment could possibly be achieved if the cross sections and their energy dependence were known accurately.

The main purpose of the simplified analysis presented is to demonstrate that the underlying idea of the phase space dynamics leads to sputtering ratios which agree approximately with the experimental observations. The theory can be extended and improved by considering additional effects and interactions as will be shown in a later publication.

References

[1] Behrisch, R., *Ergebn. Exakt. Naturw.* Vol 35, 1964, pp. 295-443.

[2] Stuart, R.V. and Wehner, G.K., *Journal of Applied Physics,* Vol. 33, 1962, pp. 2345-2352.

[3] Beebe, D.D., Nakanishi, S., and Finke, R.C., TM X-3044, 1974, NASA.

[4] Staggs, J.F., Gula, W. P., and Kerslake, W.R., *Journal of Spacecraft* Vol. 5, 1968, pp. 159-164.

[5] Kohlraush, F., *Practical Physics, III,* B.G. Teubner, Stuttgart, Germany 1968.

[6] Mott, N.F. and Massey, H.S.W., *The Theory of Atomic Collisions, Oxford University Press,* Oxford, Eng., 1965.

[7] Askerov, Sh. G. and Sena, L.A., Soviet Physics—*Solid State,* Vol. 11, 1969, pp. 1288-1292.

Roughness Induced Transition Criteria for Space Shuttle-Type Vehicles

E. Leon Morrisette*

NASA Langley Research Center, Hampton, Va.

Nomenclature

b	= semispan
M_c, M_p	= local Mach number on cone and flat plate, respectively
P	= pressure
P'	= longitudinal pressure gradient
r	= blunt body nose radius
R_k	= Reynolds number based on boundary-layer edge conditions at roughness and roughness height
$R_{x,k}$	= Reynolds number based on boundary layer edge conditions and x_k
T	= temperature
x	= longitudinal surface distance from stagnation point
x_k	= value of x at roughness location
y	= spanwise distance from centerline of body
Subscripts	
aw	= adiabatic wall
eff	= effective
t	= total
w	= wall

Received July 16, 1975; revision received December 1, 1975.

Index categories:

*Aerospace Engineer, Applied Fluid Mechanics Section, High-Speed Aerodynamics Division.

WHILE criteria exist for determining the size of three-dimensional surface roughness which will promote boundary-layer transition on simple geometric shapes,[1-3] the criteria are ill-defined for configurations with significant longitudinal and/or lateral pressure gradients (cross flow). Design of the space shuttle requires this information for sizing trips for wind-tunnel tests and for determining the effect of roughness on vehicle performance. This Note compares tripping effectiveness of roughness on a delta wing shuttle orbiter model at 20° angle of attack to that on plane and axisymmetrical bodies with and without longitudinal pressure gradients.

Two prominent parameters used in correlations of roughness induced transition are critical roughness Reynolds number[4] and effective roughness Reynolds number.[2] Critical roughness Reynolds number is a function of the flow conditions between the roughness and the "natural" transition location and probably of freestream noise. The experimental data herein are compared on the basis of effective roughness Reynolds number since this parameter is not sensitive to flow conditions downstream of the roughness. It is also believed that the effect of tunnel freestream noise on the parameter is negligible since the roughness induced disturbance dominates the transition process.[5] The effective roughness size is the smallest size roughness which causes transition to move very close to the roughness element. A compilation of effective roughness Reynolds numbers (transformed to adiabatic wall conditions) for zero pressure gradient, two-dimensional and axisymmetric flows is shown in Fig. 1 as a function of $R_{x,k}$ for various Mach numbers (faired lines, not symbols). The data were transformed to adiabatic wall conditions by using a ratio form of an equation given by Van Driest[2] which empirically accounts for the effect of wall cooling on effective roughness size

$$\frac{R_{k,eff}}{R_{k,eff,aw}} = 1 - .81 \left[\frac{T_{aw}}{T_t} - \frac{T_w}{T_t} \right] \tag{1}$$

A substantial increase in the effective roughness Reynolds number above those in zero pressure gradient at the same local flow conditions is obtained on blunt flat plates, cones, and the centerline of the shuttle model (symbols, Fig. 1, Table 1).

This effect of pressure gradient is better shown in Fig. 2. While the size parameter ratio is obviously a function of more than just pressure gradient, the effective roughness Reynolds number increases nearly an order of magnitude in the region of high-pressure gradient. The data in Fig. 2b show the same trend and allow comparison of data for which the magnitude of the pressure gradient is not available (such as the present orbiter data). The data of Fig. 2a and 2b should be considered as indicating trends and not magnitude because of the significant interpolation and extrapolation of the zero

Table 1 Key for Figs. 1 and 2

Key for figures 1 and 2					
Symbol	Configuration	M_∞	x/r	$\frac{dP}{dx}, \frac{psi}{in}$	Ref.
○	Blunt flat plate	6.0	46.0	-2.37×10^{-2}	11
○	Blunt flat plate	6.0	15.4	-2.93×10^{-2}	11
○	Blunt flat plate	6.0	15.4	-4.22×10^{-2}	11
□	Blunt cone	10.16	0.785	-3.33	9
□	Blunt cone	10.16	1.12	-1.94	9
□	Blunt cone	10.16	1.47	-0.903	9
◇	Blunt cone	10.16	0.785	-9.72	9
◇	Blunt cone	10.16	1.12	-5.89	9
◇	Blunt cone	10.16	1.47	-1.89	9
▽	Blunt cone	8.0	13.0	-1.24×10^{-2}	10
▽	Blunt cone	8.0	20.4	$+8.00 \times 10^{-4}$	10
△	Delta-wing orbiter	6.0	9	-	Present study
△	Delta-wing orbiter	6.0	18	-	Present study